MICROBIOLOGY

RESEARCH ARTICLE

Cai *et al.*, *Microbiology* 2017;163:185–196

DOI 10.1099/mic.0.000413

Lack of formylated methionyl-tRNA has pleiotropic effects on *Bacillus subtilis*

Yanfei Cai,[1,2] Pete Chandrangsu,[1] Ahmed Gaballa[1] and John D. Helmann[1,*]

Abstract

Bacteria initiate translation using a modified amino acid, *N*-formylmethionine (fMet), adapted specifically for this function. Most proteins are processed co-translationally by peptide deformylase (PDF) to remove this modification. Although PDF activity is essential in WT cells and is the target of the antibiotic actinonin, bypass mutations in the *fmt* gene that eliminate the formylation of Met-tRNA^{Met} render PDF dispensable. The extent to which the emergence of *fmt* bypass mutations might compromise the therapeutic utility of actinonin is determined, in part, by the effects of these bypass mutations on fitness. Here, we characterize the phenotypic consequences of an *fmt* null mutation in the model organism *Bacillus subtilis*. An *fmt* null mutant is defective for several post-exponential phase adaptive programmes including antibiotic resistance, biofilm formation, swarming and swimming motility and sporulation. In addition, a survey of well-characterized stress responses reveals an increased sensitivity to metal ion excess and oxidative stress. These diverse phenotypes presumably reflect altered synthesis or stability of key proteins involved in these processes.

INTRODUCTION

The protein translation machinery of bacteria differs significantly from that of eukaryotes. These differences allow the selective inhibition of bacterial growth in a eukaryotic host and are the basis for many commonly used antibiotics [1]. While the overall structure of the ribosome is conserved across the three domains of life, the differences are nevertheless sufficient to allow some ribosome-targeting antibiotics to inhibit bacterial cells with relatively little if any effect on the host translational apparatus [2]. Other antibiotics have been developed to target distinctive features of the bacterial translation machinery such as the use of a formylated initiator tRNA to initiate translation [3].

In bacteria, translation initiates with a formylated methionyl tRNA (fMet-tRNA^{fMet}) produced by methionyl-tRNA formyltransferase (FMT). The resulting fMet-tRNA^{fMet} is loaded onto the 30S subunit of the ribosome bound to mRNA to form the 30S initiation complex [4]. Subsequent addition of the 50S (large) ribosome subunit and completion of loading of the fMet-tRNA^{fMet} into the P site (with release of the initiation factors) primes the process of translation initiation. Translation leads to the production of a polypeptide bearing an N-terminal fMet residue, which is usually co-translationally processed by peptide deformylase (PDF) [5]. In many cases, depending in large part on the size of the second amino acid [6], the resulting N-terminal methionine is subsequently removed by methionine aminopeptidase (MAP). Both PDF and MAP are essential metalloenzymes, and PDF in particular has been considered an excellent target for the development of antibiotics [7–11]. The reasons why PDF and MAP are essential are not entirely clear, but the presumption is that a failure to remove the formyl group leads to a dysregulation of either protein function or stability and blocks MAP activity, which is required because some essential proteins require removal of the N-terminal Met residue in order to function [12].

We are interested in *Bacillus subtilis* as a model system for both antibiotic resistance and metal ion homeostasis. These interests have converged around the process of translation initiation since *B. subtilis*, somewhat unusually, has two functionally redundant PDF enzymes [13] and also encodes two MAP enzymes [14]. It is unclear why the cell retains these apparently redundant metalloenzymes, but one possibility is that they differ in their required metal cofactors and perhaps differ in their resistance to metal limitation or oxidative stress.

PDF is inhibited by the antibiotic actinonin [7], and it has been targeted for development of new antibacterials by multiple pharmaceutical companies [9, 15, 16]. One complication in targeting PDF with antibacterials is that resistance can arise.

Received 24 October 2016; Accepted 15 December 2016

Author affiliations: [1]Department of Microbiology, Cornell University, Ithaca, NY 14853, USA; [2]Department of Soil Science, College of Natural Resources and Environment, South China Agricultural University, Guangzhou 510642, PR China.

***Correspondence:** John D. Helmann, jdh9@cornell.edu

Keywords: translation; tRNA; peptide deformylase; formyl-Met (fMet); *Bacillus subtilis*.

Abbreviations: FMT, methionyl-tRNA formyltransferase; MAP, methionine aminopeptidase; MG, methylglyoxal; PDF, peptide deformylase.

Five supplementary figures and three supplementary tables are available with the online Supplementary Material.

Although several mechanisms have been described, one of the most frequent is the emergence of so-called Fmt bypass mutations [16–19]. In these bypass strains, translation initiates using unformylated Met-tRNA^{Met} and PDF is therefore no longer needed (Fig. 1). Bypass mutations in *folD* and *glyA*, which are required for synthesis of the FMT substrate 10-formyltetrahydrofolate, were also identified in *B. subtilis* [18]. A second complication relates to the presence of PDF in mitochondria, which initiates translation with fMet like bacteria. Indeed, impairment of this pathway due to mitochondrial mutations affecting FMT leads to a variety of human diseases associated with bioenergetic defects [20–22].

Studies in *Pseudomonas aeruginosa*, *Escherichia coli*, *Staphylococcus aureus* and *B. subtilis* have provided initial insights into the effects of *fmt* mutations on bacterial physiology. In *P. aeruginosa*, cells lacking Fmt were reported to have a modest growth rate defect [23]. In contrast, an *E. coli fmt* null mutant was severely growth impaired [24]. In *Staph. aureus*, an *fmt* mutant had a significant fitness defect *in vitro* and reduced virulence as monitored in mouse models of infection [19, 25]. Suppressor mutations in the *agrC* gene restored better growth *in vitro* for reasons not entirely clear [26]. *B. subtilis fmt* null strains were also generated as part of a study of actinonin resistance. The *fmt* null cells were insensitive to actinonin and had a significant fitness defect, but a detailed phenotypic characterization was not reported [18].

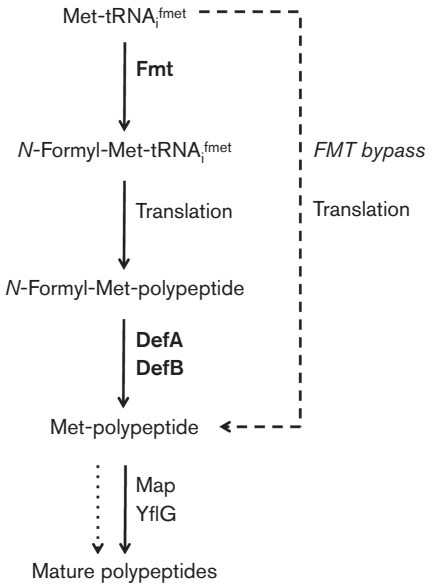

Fig. 1. Schematic diagram illustrating the roles of FMT (methionyl formylation) and the two redundant PDF enzymes (polypeptide deformylation) during bacterial translation (DefA and DefB). The dashed line indicates the use of unmodified Met-tRNA^{fMet} in initiation in the FMT bypass mutant strains. Note that some polypeptides are considered mature in the absence of removal of the initiating Met residue (dotted line).

Here, we present a survey of the phenotypic consequences arising from inactivation of *fmt* in *B. subtilis*. The *fmt* null strain is defective for several post-exponential phase adaptive programmes including biofilm formation, both swarming and swimming motility and sporulation. In addition, a survey of stress responses reveals an increased sensitivity to antibiotics, metal ion excess and oxidative stress. These diverse phenotypes presumably reflect altered synthesis or stability of key proteins involved in these processes.

METHODS

Bacterial strains and growth conditions

B. subtilis strains are derivatives of strain CU1065 and undomesticated strain NCIB 3610 [27] and are shown in Table S1 (available in the online Supplementary Material). *E. coli* strain DH5α was used for standard cloning procedures. Bacteria were grown in LB medium; where indicated, LBC medium (LB medium amended with 1 g l^{-1} of citrate trisodium dihydrate; 3.4 mM) was used. Minimal medium contained 40 mM MOPS (pH 7.4), 2 mM potassium phosphate buffer (pH 7.0), glucose (2 %, w/v), $(NH_4)_2SO_4$ (2 g l^{-1}), $MgSO_4.7H_2O$ (0.2 g l^{-1}), potassium glutamate (1 g l^{-1}), tryptophan (10 mg l^{-1}) and 80 nM $MnCl_2$. Ampicillin (100 µg ml^{-1}) was used to select *E. coli* transformants. For *B. subtilis*, antibiotics used for selection were spectinomycin (100 µg ml^{-1}), kanamycin (15 µg ml^{-1}), chloramphenicol (10 µg ml^{-1}), tetracycline (5 µg ml^{-1}) and macrolide lincosoamide/streptogramin B (contains 1 µg ml^{-1} erythromycin and 25 µg ml^{-1} lincomycin). For iron intoxication experiments, 100 mM $FeSO_4$ stocks were prepared in 0.1 N HCl, and iron was added to the indicated concentrations as described [28]. OD_{600} readings were taken on a Spectronic 21 spectrophotometer.

The *defA*::*erm* and *defB*::*erm* mutants were acquired from the *Bacillus* Knockout Erythromycin collection (B. M. Koo and C. A. Gross, University of California, San Francisco, unpublished results) maintained by the *Bacillus* Genetic Stock Center and transformed into CU1065 background. To convert the *defA*::*erm* null mutant to an unmarked, in-frame Δ*defA* mutant, the strain was transformed with pDR244 (*Bacillus* Genetic Stock Center) which encodes the Cre recombinase. The suppressed Δ*defA defB*::*erm* double mutant strains were constructed by transformation using standard techniques [29] and were confirmed by PCR to exclude strains that recovered an intact copy of *defA* by congression. PCR products were amplified for the *fmt*, *folD* and *glyA* genes and sequenced to identify possible suppressor mutations. An *fmt*::*kan* null mutant was generated by replacing the coding region with a kanamycin resistance cassette using long flanking homology PCR followed by DNA transformation as previously described [30]. Primer pairs used for PCR amplification were 6891/6892 for *fmt* (Table S2). The *fmt* complemented strains were constructed by using vector pPL82 [31]. PCR products were amplified from *B. subtilis* CU1065 chromosomal DNA, digested with endonucleases and cloned into pPL82. pPL82 contains a

chloramphenicol resistance cassette, a multiple cloning site downstream of the $P_{spac(hy)}$ promoter and the *lacI* gene between the upstream and downstream fragments of the *amyE* gene. The sequences of the inserts were verified by DNA sequencing.

Measurement of stress sensitivity

Disc diffusion assays were performed as described [32]. Briefly, strains were grown to an OD_{600} of 0.4. A 100 µl aliquot of these cultures was mixed with 4 ml of 0.75 % LB soft agar (kept at 50 °C) and directly poured onto LB plates (containing 15 ml of 1.5 % LB agar). The plates were dried for 10 min in a laminar airflow hood. Filter paper (6.5 mm) discs containing the chemicals to be tested were placed on the top of the agar, and the plates were incubated at 37 °C overnight. The overall diameter of the inhibition zones was measured along two orthogonal lines. Plates were imaged using a Chemi DocTM MP Imaging System (Bio-Rad) with white transillumination. For metal intoxication, 10 µl of the following chemicals was added to the filter paper disc: 1 M $FeSO_4$, 1 M $FeCl_3$, 100 mM $MnCl_2$, 100 mM $ZnCl_2$, 100 mM $CoCl_2$ and 100 mM $NiCl_2$. For streptonigrin sensitivity tests, $FeSO_4$ or $FeCl_3$ was added to both the soft agar and the plates to a concentration of 100 µM, and 5 µl streptonigrin (5 mg ml^{-1}) solution in DMSO was added to the filter paper discs. For sensitivity tests, antibiotics used in this study included cefuroxime (6 µg), ampicillin (20 µg), fosfomycin (250 µg), oxacillin (20 µg), vancomycin (50 µg), lysozyme (200 µg), D-cycloserine (1 mg), penicillin G (100 µg), lincomycin (250 µg), erythromycin (10 µg), spectinomycin (1 mg), tetracycline (50 µg) and methylglyoxal (MG, 50 µg). In addition, hydrogen peroxide (~2.4 µmol H_2O_2) and paraquat (2.5 µmol) were used to test the sensitivity to reactive oxygen species.

Actinonin sensitivity was measured by growth curve analysis in a Bioscreen microplate reader. Strains were grown to an OD_{600} of 0.4 in MH medium (Sigma-Aldrich). Two microlitre aliquots were inoculated in 200 µl MH medium containing 0, 0.5, 5, 10, 50 or 500 µg ml^{-1} actinonin in a Bioscreen 100-well microtitre plate. Growth was measured spectrophotometrically (OD_{600}) every 15 min for 24 h using a Bioscreen C incubator (Growth Curves USA) at 37 °C with continuous shaking.

Growth measurements

To test metal dependence of growth, 10 µM $FeCl_3$ or 5 µM $MnCl_2$ was added to the minimal medium containing 40 mM MOPS (pH 7.4), 2 mm potassium phosphate buffer (pH 7.0), 20 g l^{-1} glucose, 2 g l^{-1} $(NH_4)_2SO_4$, 0.2 g l^{-1} $MgSO_4.7H_2O$, 1 g l^{-1} potassium glutamate, 10 mg l^{-1} tryptophan and 80 nm $MnCl_2$. To test the iron sensitivity of the mutant, strains were grown to an OD_{600} of 0.4 in LB medium. Two microlitre aliquots were inoculated to 200 µl LBC medium in a Bioscreen 100-well microtitre plate. Growth was measured spectrophotometrically (OD_{600}) every 15 min for 48 h using a Bioscreen C incubator (Growth Curves USA) at 37 °C with continuous shaking.

Swarming and swimming motility assays

Swimming and swarming motility were monitored using standard assays [33, 34]. LB plates containing 0.7 and 0.3 % agar were dried in a laminar flow hood for 30 min and then spotted in the centre with 5 µl LB precultures (OD_{600} ~0.4). The plates were then dried for another 15 min and incubated overnight at 37 °C.

Biofilm and pellicle formation

To monitor pellicle formation [35], 50 µl LB preculture (OD_{600} ~0.4) was inoculated into 10 ml minimal MSgg medium [5 mM potassium phosphate (pH 7), 100 mM morpholinepropanesulfonic acid (pH 7), 2 mM $MgCl_2$, 700 µM $CaCl_2$, 50 µM $MnCl_2$, 50 µM $FeCl_3$, 1 µM $ZnCl_2$, 2 µM thiamine, 0.5 % glycerol (v/v), 0.5 % glutamate, 50 µg ml^{-1} tryptophan, 50 µg ml^{-1} phenylalanine and 50 µg ml^{-1} threonine] and incubated at 22 °C [35]. For colony architecture analysis, 5 µl of LB precultures (OD_{600} ~0.4) was spotted onto minimal MSgg agar plates (dried for 30 min in a laminar airflow prior to spotting) and incubated at 30 °C.

Monitoring sporulation progress and efficiency

For imaging sporulation, starvation was induced by resuspension [36]. Microscopy was performed using an Olympus BX61 epifluorescence microscope. Images were acquired using Cooke SensiCam and Slidebook software (Intelligent Imaging). For the sporulation assay, 0.5 ml of sporulating cells was pelleted and resuspended in 0.11 ml of the original culture medium; 2 µl of this cell suspension was placed on a slide and mixed with 1 µl of a stain mix containing 5 µg ml^{-1} FM 4-64 and 30 µg ml^{-1} MitoTracker Green FM (Molecular Probes) diluted in sporulation salts [37]. For quantitative sporulation assays, cells were grown after resuspension for 24 h with shaking at 37 °C. For spore measurements, 500 µl of cell culture was added to a new tube and heated 30 min at 80 °C and 3 µl aliquots from serial 10-fold dilutions were spotted on LB plates. The plates were incubated at 37 °C for overnight (WT) or 48 h (*fmt* mutant) to monitor sporulation efficiency.

RESULTS

Isolation and characterization of *fmt* null mutants

In ongoing work, we have sought to understand the rationale behind the presence of two, apparently redundant, PDFs in *B. subtilis*. PDF activity is required to remove the formyl group introduced into proteins by FMT (Fig. 1). The presence of such paralogous pairs of metalloenzymes is a common theme in bacterial physiology and is often associated with utilization of distinct metal cofactors [38]. In the course of these studies, we used genomic transformation to generate a *defA defB* double mutant strain (Δ*defA defB*::*erm*). After excluding those transformants that had recovered an intact copy of *defA* by congression, a small number of double mutants were recovered. We reasoned that this low frequency was likely indicative of a requirement for a suppressor mutation to allow growth in the absence of PDF.

Since prior work had indicated that inactivation of the *fmt*, *folD* and *glyA* genes can lead to actinonin resistance in *B. subtilis* [18], these three loci were sequenced in three isolates. One strain contained a frameshift mutation in *fmt* (*fmt1*), one had multiple base changes in *glyA* and the third appeared to be WT at all three loci and may therefore contain a mutation in a different locus (Table S3).

We quickly appreciated that the Δ*defA defB*::*erm fmt1* strain is pleiotropic (Figs S1–S3). For example, this strain grows more slowly than WT and is more sensitive than WT to H_2O_2, paraquat and iron intoxication. Since PDF is not required in the absence of Fmt activity, we reasoned that these phenotypes likely arise from the *fmt1* mutation and are probably unrelated to the loss of PDF. To date, there has only been one prior study of a *B. subtilis fmt* null mutant (a large in-frame deletion) recovered in a selection for actinonin resistance [18]. The mutant had a doubling time roughly twice as long as WT in MH medium and an even greater impairment in minimal media. Some changes were also noted at both the transcriptome and proteome levels, but the details were not reported. These observations all suggest that cells lacking Fmt activity are viable, but growth impaired. However, since this strain arose as a suppressor, and the whole-genome sequence was not determined (sequencing was limited to four candidate loci), we cannot exclude the possibility that some or all of these effects may have resulted from changes at other loci. Moreover, no complementation studies were performed in this prior study.

To further explore the physiological consequences of inactivating Fmt, we generated an *fmt*::*kan* null mutant (designed *fmt*) in an otherwise WT background using allelic replacement. Next, we complemented this mutation by expression of *fmt* from a plasmid integrated at the *amyE* locus (*fmt* $P_{spac(hy)}$-*fmt*). We then used this mutant strain together with its isogenic complemented strain for further physiological characterization.

An *fmt* null mutant is sensitive to H_2O_2, paraquat and methylglyoxal

The *fmt* null mutant has a significantly increased zone of growth inhibition when exposed to H_2O_2 or to paraquat, a redox-cycling dye that generates reactive oxygen species. Importantly, these phenotypes are complemented by ectopic expression of *fmt* from the $P_{spac(hy)}$ promoter (Fig. 2a). We hypothesized that alterations in the process of translation initiation in the *fmt* strain might have reduced production of the major vegetative catalase (KatA), known to be both highly abundant and a primary H_2O_2 resistance determinant [39]. However, epistasis studies suggest that the effects of Fmt and KatA on H_2O_2 resistance are additive, and therefore, the effect of Fmt cannot be due simply to decreased catalase activity (Fig. 2b). Next, we tested the hypothesis that the *fmt* mutation might affect expression of alkylhydroperoxide reductase, which is also likely to play a role in the detoxification of H_2O_2 [40]. As reported previously [41], an *ahpC* null mutant was more resistant than WT to H_2O_2, and this was shown previously to result from elevated expression of the PerR regulon including catalase. This effect of an *ahpC* mutation was still seen in the *fmt* strain (Fig. 2b), suggesting that this strain can produce elevated levels of catalase even in the absence of Fmt. Finally, we

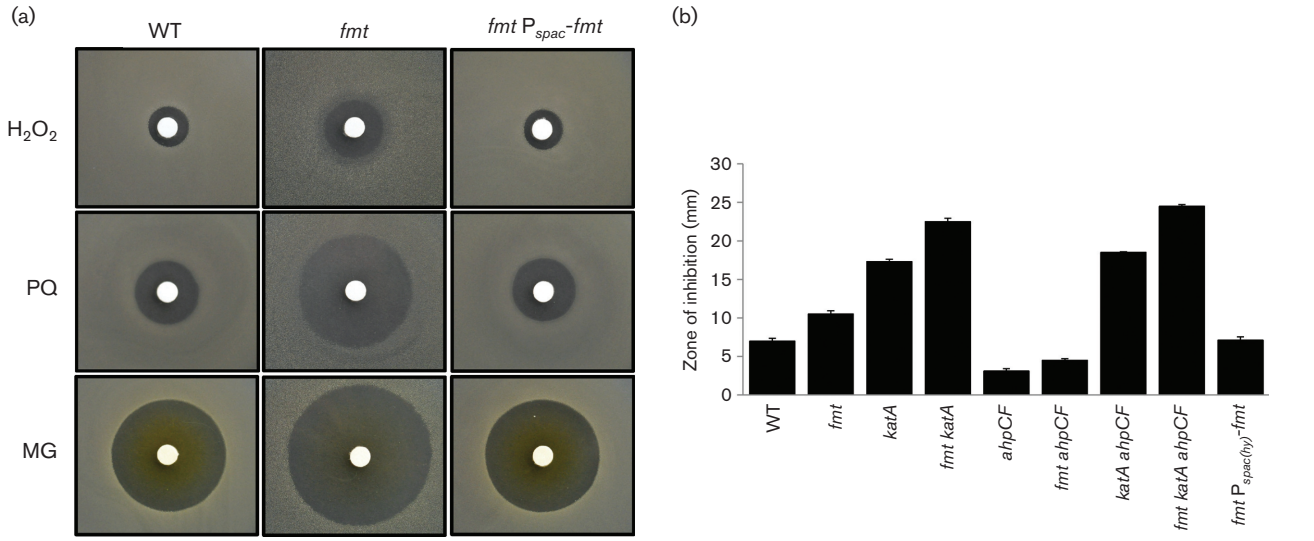

Fig. 2. An *fmt* mutant has elevated sensitivity to hydrogen peroxide, paraquat and MG stress. (a) Representative photograph (from at least six replicates) of disc diffusion assays with WT (CU1065), an *fmt* mutant (HB21006) and an *fmt* $P_{spac(hy)}$-*fmt* complemented strain (HB21016) on LB plates. The discs were spotted with hydrogen peroxide (H_2O_2, 2.4 µmol), paraquat (PQ, 2.5 µmol) or MG (27.5 µmol) as indicated. (b) Sensitivity of WT and various mutant strains to hydrogen peroxide. The results are expressed as the diameter of the inhibition zone (mm) minus the diameter of the filter paper disc (6.5 mm). The mean±SE from at least three biological replicates is reported.

note that the highly H_2O_2-sensitive *katA ahpC fmt* triple mutant is more sensitive than the *katA ahpC* double mutant, indicating that loss of Fmt affects peroxide sensitivity independently of both KatA and AhpC (Fig. 2b). Collectively, these results demonstrate that the *fmt* mutant is sensitive to H_2O_2, this defect can be complemented and it is not due to an inability of the cell to synthesize protective levels of catalase.

The *fmt* null strain also displays a dramatically increased sensitivity to the endogenously produced reactive electrophile MG (Fig. 2a). This phenotype is also complemented by the ectopic expression of *fmt*. Previous results have defined the major resistance pathways for MG which include both bacillithiol-dependent and bacillithiol-independent detoxification enzymes [42]. We used epistasis analysis to determine whether the increased MG sensitivity could be linked to decreased expression of a specific MG resistance determinant. However, introduction of an *fmt* null mutation further increased the MG sensitivity of every tested strain, including strains lacking multiple resistance pathways (Fig. S4). We therefore conclude that the sensitivity to MG in the *fmt* null strain is likely to be multifactorial and/or is independent of altered expression of known resistance pathways.

An *fmt* null mutant has altered metal ion homeostasis

The major molecular mechanisms of H_2O_2 toxicity result from cytosolic Fenton chemistry catalysed by Fe(II) [43]. As a result, mutations that elevate intracellular Fe levels may result in an increased sensitivity to H_2O_2 [28, 44]. To determine if the *fmt* mutation leads to alterations in metal ion homeostasis, we tested metal ion sensitivity using a disc diffusion assay. The *fmt* mutant displayed a significantly increased sensitivity to both Fe(II) and Fe(III), which can be complemented by expression of *fmt* from the $P_{spac(hy)}$ promoter (Fig. 3a). In contrast with Fe, there was no statistically significant change for the *fmt* null strain in sensitivity to Zn(II), Co(II) or Ni(II). However, the *fmt* null strain was dramatically increased in resistance to Mn(II) and this phenotype was reversed upon ectopic expression of *fmt* (Fig. 3b).

The molecular basis for these alterations in metal ion homeostasis in the *fmt* null mutant is not yet clear. However, iron toxicity in efflux defective cells is strongly mitigated by Mn(II) [28], and Mn(II) toxicity in efflux defective *E. coli* cells has been linked to a dysregulation of iron homeostasis [45]. Therefore, we speculate that the Mn(II) resistance noted here is due to elevated intracellular Fe(II)

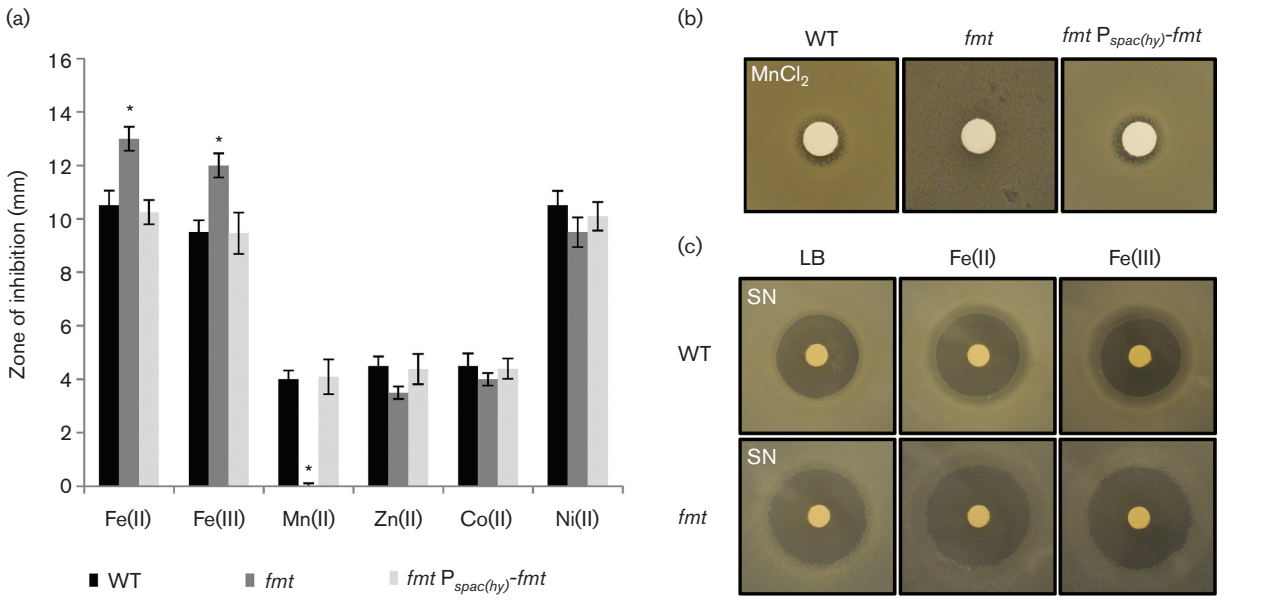

Fig. 3. An *fmt* mutant is sensitive to iron and has an increased resistance to manganese. (a) The sensitivity of WT (CU1065, black bars), an isogenic *fmt* :: *kan* mutant (HB21006, dark grey bars) and an *fmt* $P_{spac(hy)}$-*fmt* complemented strain (HB21016, light grey bars) to metal ion stress as monitored using a disc diffusion assay. The results are expressed as the diameter of the inhibition zone (mm) minus the diameter of the filter paper disc (6.5 mm). The mean±SE from at least three biological replicates is reported. Significant differences from WT and *fmt* mutant as determined by two-tailed *t*-test are indicated: *P<0.01. The discs were spotted with 10 µl of 1 M $FeSO_4$, 1M $FeCl_3$, 100 mM $MnCl_2$, 100 mM $ZnCl_2$, 100 mM $CoCl_2$ and 100 mM $NiCl_2$ separately. (b) An *fmt* mutant is more resistant to Mn(II) intoxication than WT. Representative photographs (from three replicates) of a disc diffusion assay with WT, *fmt* and *fmt* $P_{spac(hy)}$-*fmt* strains on LB plates containing a disc spotted with 10 µl of 100 mM $MnCl_2$. (c) An *fmt* null mutant displays increased sensitivity to streptonigrin (SN). Representative photographs (from three replicates) of a disc diffusion assay with WT, *fmt* and *fmt* $P_{spac(hy)}$-*fmt* strains on LB plates containing either no supplement, 100 µM $FeSO_4$ or $FeCl_3$. Each disc was spotted with 5 µl of 5 mg ml^{-1} (25 µg) SN.

levels. To determine if the *fmt* mutation leads to an elevation of intracellular Fe pools, we monitored sensitivity to streptonigrin, a quinone antibiotic whose activity is correlated with intracellular iron availability [46]. Under all conditions tested, the *fmt* null strain was more sensitive to streptonigrin, consistent with a defect in iron homeostasis and an elevation of intracellular Fe pools (Fig. 3c). The reason why iron levels are elevated is presently unclear, but it has previously been shown that a null mutation in *pfeT*, encoding an Fe(II) efflux ATPase, leads to a similar phenotype [28]. It is therefore possible that synthesis or stability of PfeT is compromised in the *fmt* null mutant strain.

An *fmt* null mutant is sensitive to citrate intoxication

While investigating iron sensitivity, we tried to grow the *fmt* strain using LB medium amended with 1 g l^{-1} of citrate to increase iron solubility (as reported previously [28]) but discovered, unexpectedly, that this strain is very sensitive to growth inhibition by citrate (Fig. 4a). This citrate sensitivity phenotype is also apparent as a greatly reduced plating efficiency on citrate-containing medium (LBC plates [28]) relative to WT in studies to test Fe(II) sensitivity, and this could be reversed by ectopic expression of *fmt* (Fig. 4b). Sensitivity to carboxylic acids was specific for citrate when monitored by disc diffusion assay (Fig. 4c) and was not observed with fumarate or succinate (data not shown). It had been noted previously that an *fmt* mutant strain was less able to grow using carboxylic acids as carbon sources, but the growth inhibition reported here is specific to citrate and is observed on rich medium, suggesting that this is not due to a defect in citrate catabolism.

Since citrate is known to be a good chelator of iron and other metals, we hypothesized that citrate sensitivity might be related to altered iron homeostasis. Citrate could act by altering metal availability in the medium or by being imported into the cell where high levels of citrate could perturb metal homeostasis. To determine if citrate toxicity required import into the cell, we tested the effect of various mutations known to affect metal homeostasis. The only mutation that reduced citrate sensitivity was *yfmC*, which inactivates an operon encoding an importer specific for iron citrate [47]. This uptake system is Fur regulated and normally expressed under iron limitation. This suggests that citrate toxicity occurs, at least in part, intracellularly. Toxicity was not fully suppressed, but citrate can also be imported through alternative citrate uptake systems including CitM and CitH [48].

An *fmt* null mutant is altered in sensitivity to antibiotics

We next examined the effects of the *fmt* mutation on susceptibility to antibiotics. As previously reported [18], the *fmt* mutant is markedly more resistant to the PDF inhibitor actinonin (Fig. 5a), since PDF is dispensable in the absence of Fmt (Fig. 1). As expected, actinonin sensitivity was restored by ectopic expression of *fmt*. Furthermore, the *fmt* mutant exhibited significantly increased sensitivity to the peptidoglycan synthesis inhibitors fosfomycin, D-cycloserine and vancomycin, but not to the β-lactam cefuroxime or penicillin (Fig. 5b). The *fmt* mutant was also increased in sensitivity to the translation inhibitors tetracycline and spectinomycin (Fig. 5b), as well as lincomycin and erythromycin (data not shown). As shown for fosfomycin and

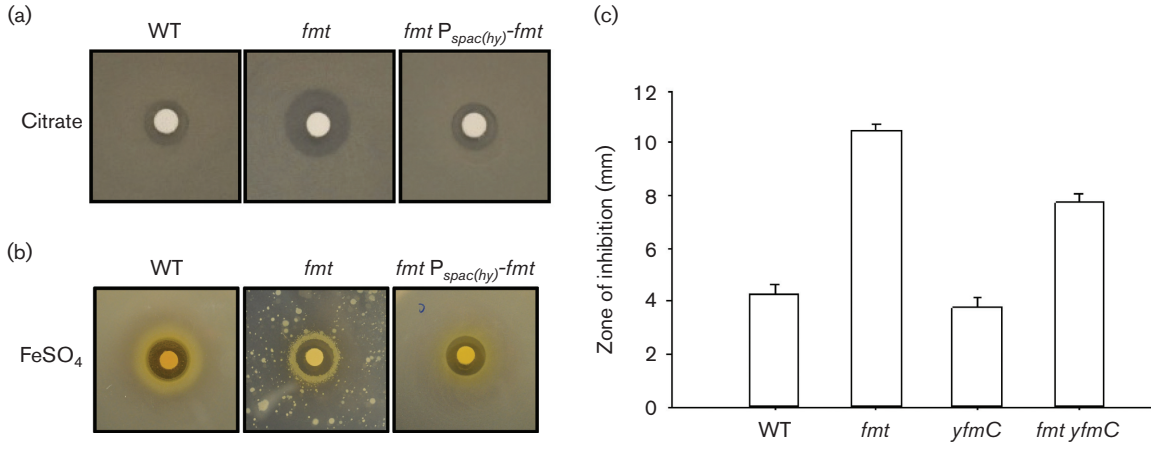

Fig. 4. An *fmt* null mutant is sensitive to citrate. (a) Representative photograph (from at least six replicates) of a disc diffusion assay with WT (CU1065), *fmt* mutant (HB21006) and *fmt* $P_{spac(hy)}$-*fmt* (HB21016) strains on LB plates. The discs were spotted with 10 µl of 1 M trisodium citrate ($Na_3C_6H_5O_7$) as indicated. (b) Growth of WT, *fmt* mutant and *fmt* $P_{spac(hy)}$-*fmt* (HB21016) strains on LBC plates (LB supplemented with 1g l^{-1} of sodium citrate) at 37 °C for 36 h. In this experiment, the discs were spotted with 10 µl of 1 M $FeSO_4$. Note that the *fmt* mutant had a severe growth defect in this medium and could not form a lawn. Note also that there is better growth near the Fe-containing filter, suggesting that citrate may impose an Fe limitation. (c) Quantitation of sensitivity of WT and mutant strains to citrate using disc diffusion assay. The results are expressed as the diameter of the inhibition zone (mm) minus the diameter of the filter paper disc (6.5 mm).

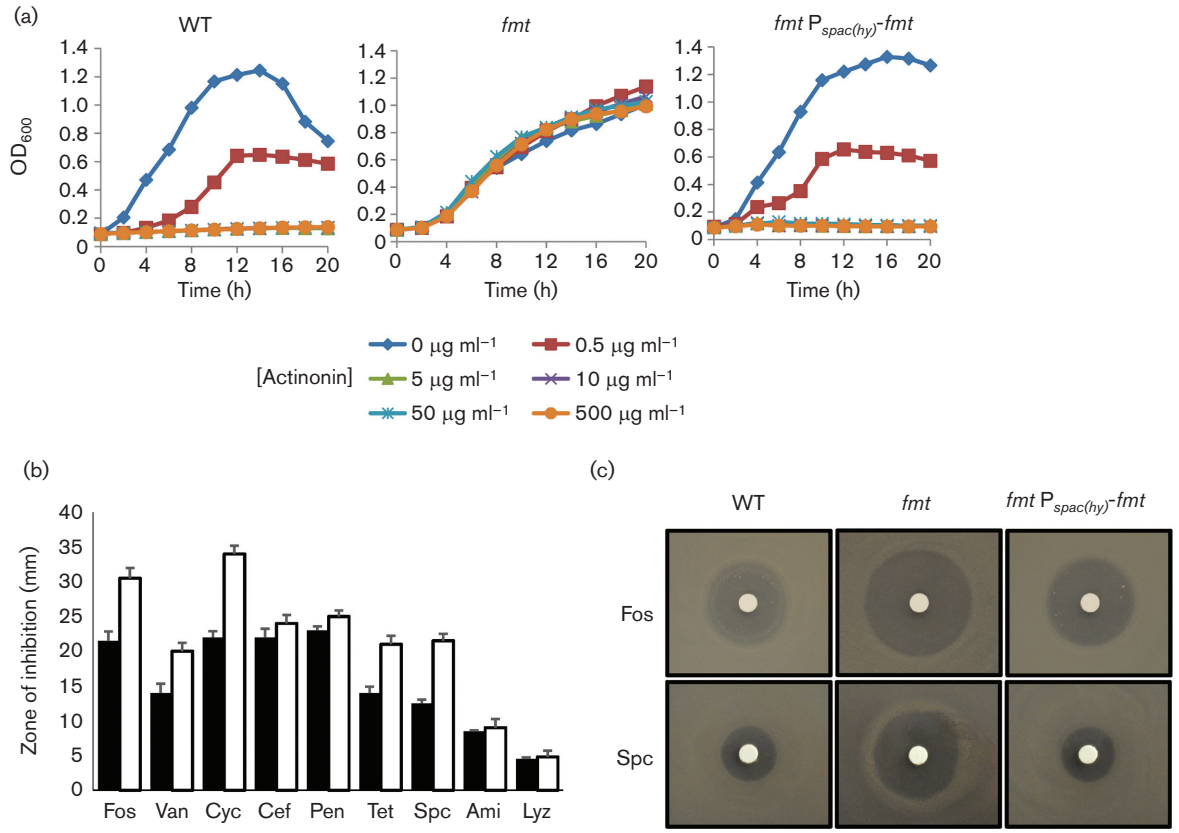

Fig. 5. An *fmt* mutant displays altered antibiotic sensitivity. (a) Sensitivity of WT, isogenic *fmt*::*kan* mutant (HB21006) and the *fmt*::*kan* P_{spac}-*fmt* (HB21016) strains to actinonin as measured by growth curve assays. Actinonin concentrations used are noted below the graph. The data shown are representative of at least three independent experiments. (b) Sensitivity of WT (black bars) and an isogenic *fmt*::*kan* mutant (HB21006, white bars) to antibiotic as monitored using a disc diffusion assay on LB plates. Antibiotics and cell envelope active agents used were fosfomycin (Fos, 250 µg), vancomycin (Van, 50 µg), D-cycloserine (Cyc, 1 mg), cefuroxime (Cef, 6 µg), penicillin G (Pen, 100 µg), tetracycline (Tet, 50 µg), spectinomycin (Spc, 0.5 mg), amitriptyline (Ami, 250 µg) and lysozyme (Lyz, 200 µg), The mean±SE from at least three biological replicates is reported. (c) Representative photographs (from at least six replicates) of a disc diffusion assay with WT or an *fmt* mutant (HB21006) and an *fmt* $P_{spac(hy)}$-*fmt* complemented strain (HB21016) cell on LB plates. The discs were spotted with fosfomycin (250 µg) or spectinomycin (0.5 mg) as indicated.

spectinomycin, the antibiotic sensitivity could be complemented by ectopic expression of *fmt* (Fig. 5c). The genetic determinants of fosfomycin resistance have been previously studied in *B. subtilis* and the major resistance determinant is the FosB bacillithiol *S*-transferase, which inactivates fosfomycin by covalent modification [49–51]. We therefore hypothesized that, perhaps, the *fmt* mutation led to a significant decrease in expression of either FosB or the enzymes required for the synthesis of the required bacillithiol cofactor [50]. However, epistasis studies did not support this hypothesis and indicate that other factors are involved (Fig. S5). The basis for these phenotypic differences awaits further investigation.

Fmt is required for swarming motility

From the analyses above, it is clear that the *fmt* mutant is pleiotropic and has affected cellular physiology and growth in diverse ways. Next, we turned our attention to the ability of the *fmt* mutant to engage in the various complex post-exponential responses that have been well characterized in *B. subtilis*. These include the activation of motility (both swimming and swarming), formation of complex structured biofilms and formation of endospores [52].

Bacteria can exhibit swimming motility in liquid media or swarming motility on surfaces. Swimming requires flagellar rotation, whereas swarming requires both flagella and the ability to form multicellular rafts [53]. To test whether Fmt is involved in swimming and swarming motility, we inoculated Petri plates containing 0.3 and 0.7 % agar ('swim plates' and 'swarm plates', respectively) [33]. For this assay, we used the undomesticated NCIB 3610 background, since the standard 168 laboratory strain does not exhibit significant motility on solid surfaces [54]. After 18 h, the WT 3610 was able to completely colonize the surface of the 0.7 % agar swarm plate, whereas the growth of the *fmt* mutant was restricted to the centre of the plate (Fig. 6), suggesting a loss of swarming motility, which requires both flagellar-based

motility and an ability of cells to bundle and form motile rafts. The *fmt* mutant clearly retains flagellar-based motility as seen by light microscopy (data not shown), suggesting that the defect may be in other factors required for swarming motility. On 0.3 % agar ('swim plates'), NCIB 3610 expands rapidly and completely through the agar within 18 h. In contrast, the *fmt* mutant exhibits complex pattern formation with branching dendrites, a very unusual phenotype for a 'swim plate' assay (Fig. 6). Both the swarming and swimming defects of the *fmt* mutant can be complemented by expression of *fmt* from an ectopic locus.

Fmt is necessary for formation of complex structured biofilms

Bacteria often exist in the environment as cell aggregates called biofilms and *B. subtilis* is a model organism to study biofilm formation [55, 56]. To assess the contribution of Fmt to this multicellular process, we monitored colony morphology on MSgg plates and pellicle formation in MSgg liquid medium. These studies were also conducted using NCIB 3610, as it forms more robust biofilms and complex colony morphology in comparison to the standard 168 laboratory strain [35]. As expected, the WT NCIB 3610 strain forms complex colony patterns on MSgg plates and robust, wrinkled pellicles on MSgg liquid medium after 2 days. In contrast, the *fmt* mutant displays reduced biofilm architecture and an unstructured pellicle in comparison to the WT strain, even after 9 days (Fig. 7).

Fmt is necessary for efficient sporulation

Spore formation is a highly regulated, complex developmental process, which allows *B. subtilis* to survive many environmental insults [57]. To test whether Fmt is involved in sporulation, the sporulation efficiency of WT and an isogenic *fmt* mutant was compared. After resuspension in sporulation-inducing medium [36] and incubation for 24 h (37 °C with shaking), non-sporulating cells were heat killed by incubation at 80 °C for 30 min. The surviving spores were enumerated after serial dilution on LB plates incubated at 37 °C (Fig. 8a). After 24 h of incubation, WT cells had a sporulation efficiency of 85±0.2 %, compared to a sporulation efficiency of 4.1±0.8 % for the *fmt* mutant, suggesting that the *fmt* mutant is oligosporogenous.

To identify the role of Fmt mutant in spore maturation, we monitored spore development by microscopy 4 and 24 h after initiation of sporulation by resuspension in sporulation medium. *B. subtilis* sporulation has seven stages (Stages I–VII) [58]. An early step in the *B. subtilis* sporulation pathway, asymmetric cell division, creates the small forespore and larger mother cell (Stage II). During the next stage of sporulation, engulfment (Stage III), the mother cell membranes move up and around the forespore. Completion of engulfment corresponds with membrane fusion resulting in the release of the forespore into the mother cell cytoplasm. After engulfment (Stages IV and V), the spore completes development within the mother cell and is released by mother cell lysis (Stages VI and VII). Cells were visualized by staining with FM 4-64 and MitoTracker Green FM [37]. Since FM 4-64 binds the cell membrane but is nonpermeable, both the membrane of the mother cell and forespore are accessible to FM 4-64 during engulfment. After engulfment is complete,

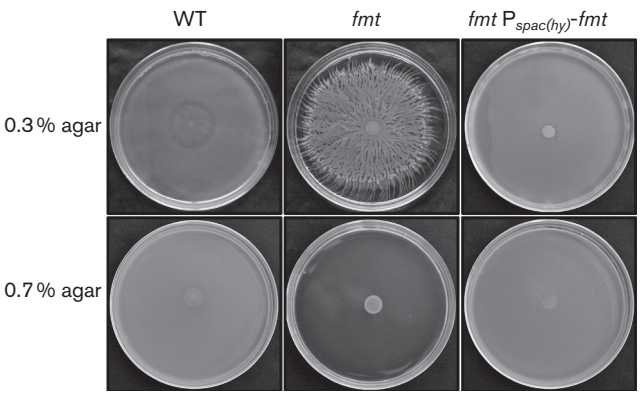

Fig. 6. An *fmt* mutant displays a swimming defect and a loss of swarming motility. Representative photographs of the NCIB 3610 WT (NCIB 3610), an isogenic *fmt* mutant (HB21009) and an *fmt* $P_{spac(hy)}$-*fmt* complemented strain (HB21017) inoculated on LB plates. A 5 µl culture from the mid logarithmic growth stage (OD_{600} ~0.4) was spotted on LB plates containing 0.3 or 0.7 % agar and incubated at 37 °C for 18 h.

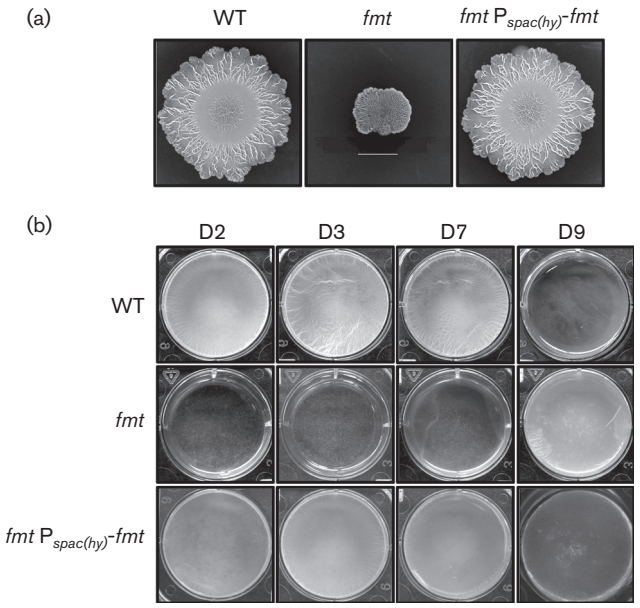

Fig. 7. An *fmt* mutant is defective in biofilm architecture and pellicle formation. (a) Representative images showing colony architecture morphology after 8 days of growth at 30 °C on MSgg plates. The WT (NCIB 3610), *fmt* (HB21009) and *fmt* $P_{spac(hy)}$-*fmt* (HB21017) strains are shown (scale bar=1 cm). (b) The pellicle formation monitored by growth at 22 °C in MSgg liquid medium at 2, 3, 7 and 9 days. The WT (NCIB 3610), *fmt* (HB21009) and *fmt* $P_{spac(hy)}$-*fmt* (HB21017) strains are shown.

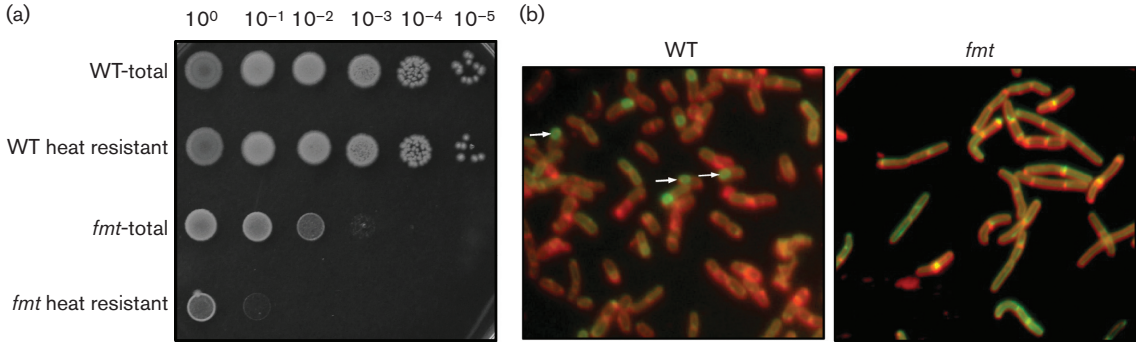

Fig. 8. The *fmt* mutant is oligosporogenous and is defective in membrane fusion. (a) The selected strains were induced to sporulate using a resuspension protocol. Efficiency of spore formation for WT (CU1065) and an isogenic *fmt* mutant (HB21006) was monitored by plating 3 µl of 10-fold cell dilutions (left to right; 10^0 to 10^{-5}) with and without treatment at 80 °C for 30 min to inactivate vegetative cells and was then incubated at 37 °C for 24 h. The photograph is representative of three biological replicates. Additional growth is seen on the *fmt* plate after 48 h, but there is still a nearly 100-fold reduction in colonies after heating as before, consistent with a low frequency of successful sporulation. (b) Sporulation progress for the WT and *fmt* mutant as monitored 4 h after resuspension using a membrane fusion assay with staining with FM 4-64 and MitoTracker Green [37]. The arrows (left panel) indicate cells that have completed engulfment and membrane fusion, as indicated by the green staining. In the right panel, cells stain with both dyes, indicative of a block at the membrane fusion step (similar results were seen after 24 h, with cells that had engulfed the forespore but had been blocked in membrane fusion).

only the mother cell membrane stains with FM 4-64 and the membrane-permeable MitoTracker Green FM selectively stains green the fully engulfed forespore after membrane fusion (Fig. 8b, arrows). We monitored sporulation of over 1000 cells at 4 and 24 h following the onset of sporulation. In WT, membrane fusion and completion of engulfment was evident after 4 h of sporulation (Table 1, Fig. 8) and the majority of the cells (84 %) had completed sporulation after 24 h. In contrast, the *fmt* mutant failed to complete membrane fusion and engulfment after 4 h. Furthermore, after 24 h, 87 % of the *fmt* mutant cells had initiated membrane migration, yet only a small fraction (6 %) were able to complete engulfment, indicating that an *fmt* mutant is defective, rather than delayed, for sporulation. In total, these data suggest that, in the absence of Fmt, the final stage of engulfment (membrane fusion) is inefficient.

DISCUSSION

Roles of PDF and FMT in bacterial translation

Translation in bacteria differs from that of the eukaryal cytosol in several key features [4]. Of particular relevance to this study, initiation begins with a specialized tRNA, the fMet-tRNA^{fMet}. This initiator tRNA is first aminoacylated by the methionyl-tRNA synthetase and then the methionyl residue is formylated by FMT. The majority of polypeptides are subsequently deformylated by PDF in a co-translational process. Inhibition of PDF leads to cell death [7], but suppressors often emerge that have inactivated FMT (FMT bypass; Fig. 1) [19]. These findings suggest that cells are viable, albeit growth impaired, if forced to initiate translation with Met-tRNA^{fMet} (no methionyl formylation), but are inviable if proteins are synthesized with an N-terminal fMet residue that cannot be deformylated.

Use of a formylated initiator tRNA is thought to confer substantial benefits on the efficiency of the translation initiation reaction. Specifically, formylation increases the interaction of fMet-tRNA^{fMet} with initiation factor 2 while blocking recognition by EF-Tu, and it facilitates loading into the ribosomal P site [4]. Protein N-terminal formylation may also play a regulatory role by serving as a signal for protein degradation [12]. Finally, it has been suggested that the use of fMet for initiation may help to coordinate translation activity with the overall metabolic status of the cell as reflected in the activity of the methionyl biosynthesis enzymes and the status of the tetrahydrofolate pool [4]. In the case of mitochondria, where the endogenously synthesized proteome is comparatively limited, formylmethionine has been shown to be required for the efficient incorporation of COX1 into respiratory complexes [20]. An analogous critical role for formylation has not been demonstrated for bacterial proteins, and formylation cannot be essential as evidenced by the viability of FMT bypass mutations.

Since PDF has been aggressively pursued as a target for new antibacterials (e.g. LBM415 from Novartis and GSK1322322 from Glaxo SmithKline), possible bypass mutations, and their implications for antibiotic efficacy, have been well studied in pathogenic organisms. In both *Staph. aureus* and *Streptococcus pyogenes*, *fmt* null mutations were the most frequent causes of resistance to PDF inhibitors [15, 19]. However, emergence of suppressor strains lacking *fmt* activity might not affect antibiotic efficacy if the resulting strains have a significant fitness defect or are compromised in virulence. Another major mechanism of resistance is either amplication of the *def* gene encoding PDF, as seen in *Haemophilus influenzae* [16], or the emergence of resistant mutations in *def*, as noted in *Staph. aureus* and *Streptococcus pneumoniae* [15, 59].

Table 1. Sporulation phenotypes of WT versus *fmt* mutant

Scoring of different sporulation phenotypes (number of cells) of WT and *fmt* at 4 and 24 h after initiation of sporulation by resuspension. Membrane migration associating with engulfment of the forespore to generate sporangia (a cell in the process of sporulation) was monitored by membrane staining. Polar septa (%) indicates the percentage of polar septa relative to total cells.

Phenotype	No. of cells			
	WT 4 h	*fmt* 4 h	WT 24 h	*fmt* 24 h
Flat polar septa	177	240	0	89
Engulfing	400	76	0	0
Membrane migration complete	181	186	163	1078
Engulfment complete	89	0	857	76
Not sporulating	228	638	0	0
Total sporangia	847	502	1020	1243
Total cells	1075	1140	1020	1243
Polar septa (%)	12	16	0	7
Engulfing (%)	37	7	0	0
Complete migration (%)	17	16	16	87
Complete engulfment (%)	8	0	84	6

Diverse effects of *fmt* inactivation in bacteria

The consequences of inactivating *fmt* appear to vary significantly between strains. *E. coli fmt* mutants were reported to be severely compromised for growth [24], whereas *P. aeruginosa* had a more modest defect [23]. *Staph. aureus fmt* mutants were also growth defective [19] and, intriguingly, severely affected in the expression of pathogenicity determinants [25]. The origins of these effects are largely unexplained but presumably result from altered translation initiation leading to reduced expression of specific proteins, although why some proteins might be less able to initiate using Met instead of fMet is not understood.

As might be expected for mutations leading to a growth defect, *fmt* null strains frequently generate suppressed strains that have increased fitness. In *Salmonella enterica*, suppression was mediated in some strains by an amplification of the genes encoding the methionyl-initiator tRNA [60]. This increase in gene dosage was postulated to help facilitate translation initiation using unmodified Met-tRNA^{Met} in place of the fMet-tRNA^{Met} that is normally used. Alternatively, mutations can arise in initiation factor 2 that increase the ability of translation to initiate using unmodified tRNA [61]. Mutations that increased fitness of *Staph. aureus fmt* null mutants were identified in *agrC* encoding an accessory gene regulator involved in quorum sensing and virulence [26]. In *P. aeruginosa*, mutation of *fmt* led to upregulation of the MexXY efflux pump [17]. These observations all suggest that cells lacking Fmt activity are viable, but growth impaired due to defects in translation activity and possible effects on protein stability. In many of these studies, the analysed *fmt* mutations arose as suppressors that give rise to resistance to PDF inhibitors. In general, it is unclear whether or not the *fmt* mutation was the only mutation in the resulting strains, and with one exception [62], complementation studies were not reported.

Effects of an *fmt* null mutation on *B. subtilis* physiology

We have sought to define the physiological consequences of a lack of methionyl formylation in *B. subtilis*. The effect of an *fmt* mutation in an actinonin-resistant *B. subtilis* isolate was addressed in a previous report, which noted general growth defects in a variety of media and effects on the transcriptome, but did not unambiguously link these phenotypes to the loss of FMT [18]. In principle, transcriptomics is a potentially useful approach since the appearance of specific stress signatures might provide clues to the consequences of translational dysregulation in cells obligately initiating translation with unmodified Met. However, the reported results were interpreted as indicating no significant transcriptome differences (as stated in the Abstract of [18]) with, paradoxically, more than 300 genes altered by more than twofold. However, no details were included as to the precise identity of these genes [18]. One can also imagine using a global proteomics approach to monitor the effects of an *fmt* mutation, as reported in a study of an *Staph. aureus fmt* bypass strain [63]. However, this approach is also limited since there are changes in the absolute levels of numerous proteins, and it is not obvious how these changes can be linked to physiologically significant variations.

Here, we chose instead to survey a variety of growth and stress-related phenotypes, including post-exponential phase adaptive processes such as motility, biofilm formation and sporulation. By focusing on well-studied but complex processes, we reasoned that it might be possible to link defects due to a loss of FMT activity to altered translation of specific protein targets and thereby provide insights into why FMT is more important for some processes (and for some organisms) than for others. Our results clearly indicate that cells lacking FMT are able to sustain growth but are defective in their resistance to stress and in their ability to engage in a variety of adaptive processes. While we have sought to link

these phenotypes to specific proteins, our epistasis results to date imply that the effects are, perhaps not surprisingly, multifactorial. Nevertheless, we suggest that further investigation of these processes may yet reveal well-defined and specific examples of proteins whose function is specifically impaired in the absence of the normal fMet-dependent initiation process. The effects of the of the *fmt* mutation may be largely due to differences in the relative amounts of specific protein products, rather than due to an absence of any specific product. The ability of *B. subtilis* to grow in the face of a globally altered proteomic landscape is a testament to the robust nature of bacterial metabolism. However, the dramatic impairment noted in motility, biofilm formation and sporulation suggests that these processes are sensitive to the presumably altered levels and ratios of their many participant proteins.

Funding information
Research reported in this publication was supported by the National Institute of General Medical Sciences of the National Institutes of Health under award numbers GM047446 and GM059323 (J. D. H) and by a grant from the National Natural Science Foundation of China (41471214) to Y. C.

Acknowledgements
We thank H. Pi for technical advice and Dr E. Angert (Cornell University) for sharing her microscope and for detailed advice and guidance on analysing sporulation-related phenotypes.

Conflicts of interest
The authors declare that there are no conflicts of interest.

References

1. **Wilson DN.** Ribosome-targeting antibiotics and mechanisms of bacterial resistance. *Nat Rev Microbiol* 2014;12:35–48.
2. **Arenz S, Wilson DN.** BLAST from the past: reassessing forgotten translation inhibitors, antibiotic selectivity, and resistance mechanisms to aid drug development. *Mol Cell* 2016;61:3–14.
3. **Brandi L, Fabbretti A, La Teana A, Abbondi M, Losi D *et al.*** Specific, efficient, and selective inhibition of prokaryotic translation initiation by a novel peptide antibiotic. *Proc Natl Acad Sci USA* 2006;103:39–44.
4. **Gualerzi CO, Pon CL.** Initiation of mRNA translation in bacteria: structural and dynamic aspects. *Cell Mol Life Sci* 2015;72:4341–4367.
5. **Sandikci A, Gloge F, Martinez M, Mayer MP, Wade R *et al.*** Dynamic enzyme docking to the ribosome coordinates N-terminal processing with polypeptide folding. *Nat Struct Mol Biol* 2013;20:843–850.
6. **Hirel PH, Schmitter MJ, Dessen P, Fayat G, Blanquet S.** Extent of N-terminal methionine excision from *Escherichia coli* proteins is governed by the side-chain length of the penultimate amino acid. *Proc Natl Acad Sci USA* 1989;86:8247–8251.
7. **Chen DZ, Patel DV, Hackbarth CJ, Wang W, Dreyer G *et al.*** Actinonin, a naturally occurring antibacterial agent, is a potent deformylase inhibitor. *Biochemistry* 2000;39:1256–1262.
8. **Olaleye OA, Bishai WR, Liu JO.** Targeting the role of N-terminal methionine processing enzymes in *Mycobacterium tuberculosis*. *Tuberculosis* 2009;89:S55–S59.
9. **Sharma A, Khuller GK, Sharma S.** Peptide deformylase – a promising therapeutic target for tuberculosis and antibacterial drug discovery. *Expert Opin Ther Targets* 2009;13:753–765.
10. **Helgren TR, Wangtrakuldee P, Staker BL, Hagen TJ.** Advances in bacterial methionine aminopeptidase inhibition. *Curr Top Med Chem* 2016;16:397–414.
11. **Leeds JA, Dean CR.** Peptide deformylase as an antibacterial target: a critical assessment. *Curr Opin Pharmacol* 2006;6:445–452.
12. **Piatkov KI, Vu TT, Hwang CS, Varshavsky A.** Formyl-methionine as a degradation signal at the N-termini of bacterial proteins. *Microb Cell* 2015;2:376–393.
13. **Haas M, Beyer D, Gahlmann R, Freiberg C.** YkrB is the main peptide deformylase in *Bacillus subtilis*, a eubacterium containing two functional peptide deformylases. *Microbiology* 2001;147:1783–1791.
14. **You C, Lu H, Sekowska A, Fang G, Wang Y *et al.*** The two authentic methionine aminopeptidase genes are differentially expressed in *Bacillus subtilis*. *BMC Microbiol* 2005;5:57.
15. **Min S, Ingraham K, Huang J, McCloskey L, Rilling S *et al.*** Frequency of spontaneous resistance to peptide deformylase inhibitor GSK1322322 in *Haemophilus influenzae*, *Staphylococcus aureus*, *Streptococcus pyogenes*, and *Streptococcus pneumoniae*. *Antimicrob Agents Chemother* 2015;59:4644–4652.
16. **Dean CR, Narayan S, Richards J, Daigle DM, Esterow S *et al.*** Reduced susceptibility of *Haemophilus influenzae* to the peptide deformylase inhibitor LBM415 can result from target protein overexpression due to amplified chromosomal *def* gene copy number. *Antimicrob Agents Chemother* 2007;51:1004–1010.
17. **Caughlan RE, Sriram S, Daigle DM, Woods AL, Buco J *et al.*** Fmt bypass in *Pseudomonas aeruginosa* causes induction of MexXY efflux pump expression. *Antimicrob Agents Chemother* 2009;53:5015–5021.
18. **Duroc Y, Giglione C, Meinnel T.** Mutations in three distinct loci cause resistance to peptide deformylase inhibitors in *Bacillus subtilis*. *Antimicrob Agents Chemother* 2009;53:1673–1678.
19. **Margolis PS, Hackbarth CJ, Young DC, Wang W, Chen D *et al.*** Peptide deformylase in *Staphylococcus aureus*: resistance to inhibition is mediated by mutations in the formyltransferase gene. *Antimicrob Agents Chemother* 2000;44:1825–1831.
20. **Hinttala R, Sasarman F, Nishimura T, Antonicka H, Brunel-Guitton C *et al.*** An N-terminal formyl methionine on COX 1 is required for the assembly of cytochrome *c* oxidase. *Hum Mol Genet* 2015;24:4103–4113.
21. **Sinha A, Köhrer C, Weber MH, Masuda I, Mootha VK *et al.*** Biochemical characterization of pathogenic mutations in human mitochondrial methionyl-tRNA formyltransferase. *J Biol Chem* 2014;289:32729–32741.
22. **Tucker EJ, Hershman SG, Köhrer C, Belcher-Timme CA, Patel J *et al.*** Mutations in MTFMT underlie a human disorder of formylation causing impaired mitochondrial translation. *Cell Metab* 2011;14:428–434.
23. **Newton DT, Creuzenet C, Mangroo D.** Formylation is not essential for initiation of protein synthesis in all eubacteria. *J Biol Chem* 1999;274:22143–22146.
24. **Guillon JM, Mechulam Y, Schmitter JM, Blanquet S, Fayat G.** Disruption of the gene for Met-tRNA(fMet) formyltransferase severely impairs growth of *Escherichia coli*. *J Bacteriol* 1992;174:4294–4301.
25. **Lewandowski T, Huang J, Fan F, Rogers S, Gentry D *et al.*** *Staphylococcus aureus* formyl-methionyl transferase mutants demonstrate reduced virulence factor production and pathogenicity. *Antimicrob Agents Chemother* 2013;57:2929–2936.
26. **Zorzet A, Andersen JM, Nilsson AI, Møller NF, Andersson DI.** Compensatory mutations in *agrC* partly restore fitness in vitro to peptide deformylase inhibitor-resistant *Staphylococcus aureus*. *J Antimicrob Chemother* 2012;67:1835–1842.
27. **McLoon AL, Guttenplan SB, Kearns DB, Kolter R, Losick R.** Tracing the domestication of a biofilm-forming bacterium. *J Bacteriol* 2011;193:2027–2034.
28. **Guan G, Pinochet-Barros A, Gaballa A, Patel SJ, Argüello JM *et al.*** PfeT, a P_{1B4}-type ATPase, effluxes ferrous iron and protects *Bacillus subtilis* against iron intoxication. *Mol Microbiol* 2015;98:787–803.

29. **Harwood CR, Cutting SM (editors)**. *Molecular Biological Methods for Bacillus*. Chichester: John Wiley and Sons; 1990.
30. **Mascher T, Margulis NG, Wang T, Ye RW, Helmann JD.** Cell wall stress responses in *Bacillus subtilis*: the regulatory network of the bacitracin stimulon. *Mol Microbiol* 2003;50:1591–1604.
31. **Quisel JD, Burkholder WF, Grossman AD.** *In vivo* effects of sporulation kinases on mutant Spo0A proteins in *Bacillus subtilis*. *J Bacteriol* 2001;183:6573–6578.
32. **Mascher T, Hachmann AB, Helmann JD.** Regulatory overlap and functional redundancy among *Bacillus subtilis* extracytoplasmic function sigma factors. *J Bacteriol* 2007;189:6919–6927.
33. **Kearns DB, Losick R.** Swarming motility in undomesticated *Bacillus subtilis*. *Mol Microbiol* 2003;49:581–590.
34. **Morales-Soto N, Anyan ME, Mattingly AE, Madukoma CS, Harvey CW *et al.*** Preparation, imaging, and quantification of bacterial surface motility assays. *J Vis Exp* 2015;98.
35. **Branda SS, González-Pastor JE, Ben-Yehuda S, Losick R, Kolter R.** Fruiting body formation by *Bacillus subtilis*. *Proc Natl Acad Sci USA* 2001;98:11621–11626.
36. **Sterlini JM, Mandelstam J.** Commitment to sporulation in *Bacillus subtilis* and its relationship to development of actinomycin resistance. *Biochem J* 1969;113:29–37.
37. **Sharp MD, Pogliano K.** An *in vivo* membrane fusion assay implicates SpoIIIE in the final stages of engulfment during *Bacillus subtilis* sporulation. *Proc Natl Acad Sci USA* 1999;96:14553–14558.
38. **Merchant SS, Helmann JD.** Elemental economy: microbial strategies for optimizing growth in the face of nutrient limitation. *Adv Microb Physiol* 2012;60:91–210.
39. **Zuber P.** Management of oxidative stress in *Bacillus*. *Annu Rev Microbiol* 2009;63:575–597.
40. **Seaver LC, Imlay JA.** Alkyl hydroperoxide reductase is the primary scavenger of endogenous hydrogen peroxide in *Escherichia coli*. *J Bacteriol* 2001;183:7173–7181.
41. **Bsat N, Chen L, Helmann JD.** Mutation of the *Bacillus subtilis* alkyl hydroperoxide reductase (*ahpCF*) operon reveals compensatory interactions among hydrogen peroxide stress genes. *J Bacteriol* 1996;178:6579–6586.
42. **Chandrangsu P, Dusi R, Hamilton CJ, Helmann JD.** Methylglyoxal resistance in *Bacillus subtilis*: contributions of bacillithiol-dependent and independent pathways. *Mol Microbiol* 2014; 91:706–715.
43. **Imlay JA.** The molecular mechanisms and physiological consequences of oxidative stress: lessons from a model bacterium. *Nat Rev Microbiol* 2013;11:443–454.
44. **Faulkner MJ, Helmann JD.** Peroxide stress elicits adaptive changes in bacterial metal ion homeostasis. *Antioxid Redox Signal* 2011;15:175–189.
45. **Martin JE, Waters LS, Storz G, Imlay JA.** The *Escherichia coli* small protein MntS and exporter MntP optimize the intracellular concentration of manganese. *PLoS Genet* 2015;11:e1004977.
46. **Yeowell HN, White JR.** Iron requirement in the bactericidal mechanism of streptonigrin. *Antimicrob Agents Chemother* 1982; 22:961–968.
47. **Ollinger J, Song KB, Antelmann H, Hecker M, Helmann JD.** Role of the Fur regulon in iron transport in *Bacillus subtilis*. *J Bacteriol* 2006;188:3664–3673.
48. **Boorsma A, van der Rest ME, Lolkema JS, Konings WN.** Secondary transporters for citrate and the Mg^{2+}-citrate complex in *Bacillus subtilis* are homologous proteins. *J Bacteriol* 1996;178: 6216–6222.
49. **Cao M, Bernat BA, Wang Z, Armstrong RN, Helmann JD.** FosB, a cysteine-dependent fosfomycin resistance protein under the control of sigma(W), an extracytoplasmic-function sigma factor in *Bacillus subtilis*. *J Bacteriol* 2001;183:2380–2383.
50. **Gaballa A, Newton GL, Antelmann H, Parsonage D, Upton H *et al.*** Biosynthesis and functions of bacillithiol, a major low-molecular-weight thiol in *Bacilli*. *Proc Natl Acad Sci USA* 2010;107:6482–6486.
51. **Lamers AP, Keithly ME, Kim K, Cook PD, Stec DF *et al.*** Synthesis of bacillithiol and the catalytic selectivity of FosB-type fosfomycin resistance proteins. *Org Lett* 2012;14:5207–5209.
52. **Kovács ÁT.** Bacterial differentiation via gradual activation of global regulators. *Curr Genet* 2016;62:125–128.
53. **Kearns DB.** A field guide to bacterial swarming motility. *Nat Rev Microbiol* 2010;8:634–644.
54. **Kearns DB, Chu F, Rudner R, Losick R.** Genes governing swarming in *Bacillus subtilis* and evidence for a phase variation mechanism controlling surface motility. *Mol Microbiol* 2004;52:357–369.
55. **Cairns LS, Hobley L, Stanley-Wall NR.** Biofilm formation by *Bacillus subtilis*: new insights into regulatory strategies and assembly mechanisms. *Mol Microbiol* 2014;93:587–598.
56. **Mielich-Süss B, Lopez D.** Molecular mechanisms involved in *Bacillus subtilis* biofilm formation. *Environ Microbiol* 2015;17:555–565.
57. **Tan IS, Ramamurthi KS.** Spore formation in *Bacillus subtilis*. *Environ Microbiol Rep* 2014;6:212–225.
58. **Errington J.** Regulation of endospore formation in *Bacillus subtilis*. *Nat Rev Microbiol* 2003;1:117–126.
59. **Margolis P, Hackbarth C, Lopez S, Maniar M, Wang W *et al.*** Resistance of *Streptococcus pneumoniae* to deformylase inhibitors is due to mutations in *defB*. *Antimicrob Agents Chemother* 2001;45: 2432–2435.
60. **Nilsson AI, Zorzet A, Kanth A, Dahlström S, Berg OG *et al.*** Reducing the fitness cost of antibiotic resistance by amplification of initiator tRNA genes. *Proc Natl Acad Sci USA* 2006;103:6976–6981.
61. **Zorzet A, Pavlov MY, Nilsson AI, Ehrenberg M, Andersson DI.** Error-prone initiation factor 2 mutations reduce the fitness cost of antibiotic resistance. *Mol Microbiol* 2010;75:1299–1313.
62. **Mader D, Liebeke M, Winstel V, Methling K, Leibig M *et al.*** Role of N-terminal protein formylation in central metabolic processes in *Staphylococcus aureus*. *BMC Microbiol* 2013;13:7.
63. **Plikat U, Voshol H, Dangendorf Y, Wiedmann B, Devay P *et al.*** From proteomics to systems biology of bacterial pathogens: approaches, tools, and applications. *Proteomics* 2007;7:992–1003.

Edited by: J. Stülke and T. Msadek